Cosmological constraints on atomic dark matter

Ellie Hughes,[1, *] Francis-Yan Cyr-Racine,[2] Fei Ge,[3] and Lloyd Knox[3]

[1]*Department of Physics, Bryn Mawr College, Bryn Mawr, Pennsylvania 19010, USA*
[2]*Department of Physics and Astronomy, University of New Mexico, Albuquerque, New Mexico 87106, USA*
[3]*Department of Physics and Astronomy, University of California, Davis, California 95616, USA*
(Dated: January 31, 2023)

An atomic dark matter model, consisting of self-interacting "dark protons," "dark electrons," and "dark photons," as explored by Cyr-Racine and Sigurdson (2013), is observationally viable, provides new observational signatures beyond non-interacting cold dark matter, and might provide a solution to the Hubble tension and to the σ_8 tension. We present updates to constraints on the model from cosmic microwave background (CMB) and baryon acoustic oscillation (BAO) data, both with and without Cepheid-calibrated supernovae constraints on the Hubble constant H_0, as well as with and without big bang nucleosynthesis (BBN) constraints on helium abundance. We set limits, in these different scenarios, on the fraction of dark matter that could be atomic dark matter. We also find that lower values of σ_8 are allowed with lower dark photon temperature.

I. INTRODUCTION

Although ΛCDM (see e.g. [1]) is currently the most widely accepted model of cosmology and is the benchmark to which all other cosmological models are compared, there are several discrepancies between values of key cosmological parameters calculated from observations of the cosmic microwave background (CMB) and more direct measurements of these parameters at low redshift. The most notable of these tensions are between different measurements of the Hubble constant H_0 and different measurements of matter fluctuation amplitude σ_8, which is defined via

$$\sigma_8^2 = \left(\frac{3}{4\pi(8h^{-1}\,\mathrm{Mpc})^3}\right)^2 \int \frac{k^3 P(k)}{2\pi} |W(k)|^2 \frac{dk}{k}, \quad (1)$$

where $W(k)$ is the Fourier transform of the "top hat" window function

$$W(r) = \begin{cases} 1 & r \leq 8h^{-1}\,\mathrm{Mpc} \\ 0 & r > 8h^{-1}\,\mathrm{Mpc}, \end{cases} \quad (2)$$
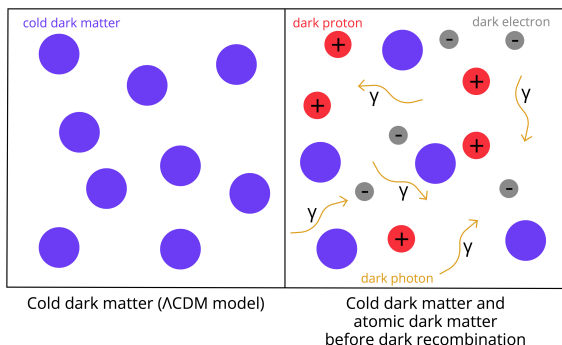
FIG. 1: Visual comparison of ΛCDM and atomic dark matter models before dark recombination.

---

* ehughes1@brynmawr.edu

k is the wavenumber, $h = H_0/(100\ \mathrm{km\ s^{-1}\ Mpc^{-1}})$, and $P(k)$ is the matter power [2].

The more statistically significant of these two tensions is the H_0 tension. Assuming standard ΛCDM cosmology, a combination of CMB observations from SPT-3G, *Planck*, and ACT find $H_0 = (67.49 \pm 0.53)\ \mathrm{km\ s^{-1}\ Mpc^{-1}}$ [3–5]. This result is in 5σ tension with the SH0ES measurement of $H_0 = (73.04 \pm 1.04)\ \mathrm{km\ s^{-1}\ Mpc^{-1}}$ from Cepheid-calibrated supernovae [6]. For a more complete description of the H_0 tension, see e.g. [7–11].

Another important cosmological tension is the σ_8 tension. Again assuming standard ΛCDM cosmology, CMB observations from *Planck* find $\sigma_8 = 0.811 \pm 0.006$ [4]. However, via measurements of cosmic shear, KiDS-1000 finds $\sigma_8 = 0.766^{+0.025}_{-0.020}$ [12]. Although these two measurements are only in $\sim 3\sigma$ disagreement, the σ_8 tension also represents a key discrepancy and could point to underlying problems with ΛCDM as the standard model of cosmology. For additional information on the σ_8 tension, see e.g. [7, 11, 13].

Since the calculation of the values of cosmological parameters from CMB measurements is highly model-dependent, in order to resolve the above-described H_0 and σ_8 tensions, it may be necessary to consider extensions to the ΛCDM model. In ΛCDM, dark matter is cold and interacts only gravitationally, both with itself and with standard model particles. Therefore, one possible avenue to extend ΛCDM is through the consideration of alternative models of dark matter.

The extension to ΛCDM that we will consider in this paper 1) allows for additional free-streaming light degrees of freedom and 2) allows for a small fraction of the total dark matter to be "atomic," consisting of "dark protons," "dark electrons," and "dark photons," which self-interact much like standard model protons, electrons, and photons. The remaining dark matter is cold dark matter, as in ΛCDM. See Fig. 1 for a visual comparison of ΛCDM dark matter and atomic dark matter. For a more complete description of the atomic dark matter model we will explore, see [14].

Atomic dark matter is observationally viable [8, 14,

15], provides new observational signatures beyond non-interacting cold dark matter, and might provide a solution to the Hubble tension [8, 16] and the σ_8 tension [16]. However, the model has not yet been fully constrained and inconsistencies related to the primordial abundance of helium and deuterium persist [8].

This paper explores an expanded model space to provide updated constraints on the atomic dark matter model using CMB and baryon acoustic oscillation (BAO) data, both with and without Cepheid-calibrated supernovae constraints on the Hubble constant H_0, as well as with and without big bang nucleosynthesis (BBN) constraints on the helium abundance. In addition to further constraining the atomic dark matter model, we discover one unexpected possible solution to the σ_8 tension.

This paper is organized as follows: In Sec. II, we outline the parameter space explored. In Sec. III, we detail the datasets used to constrain the parameters outlined in Sec. II. In Sec. IV, we present the constraints placed by current data on atomic dark matter parameters, including an unexpected allowed region of low σ_8 and low dark photon temperature. In Sec. V, we confirm the observational viability of this unexpected allowed region and explore its impacts on matter power spectra and CMB power spectra. In Sec. VI, we summarize and conclude.

II. MODEL SPACE

In this paper, we present constraints on an expanded atomic dark matter parameter space. In addition to the standard ΛCDM parameters (H_0, $\Omega_b h^2$, $\Omega_c h^2$, τ, A_s, and n_s), we vary the fraction of atomic dark matter $f_{\rm adm}$, the temperature of dark photons today $T_{d\gamma}^0$, the binding energy of dark hydrogen $B_d = \alpha_d m_{de}/2$, and the effective number of relativistic species $N_{\rm eff}$. For more information on the ΛCDM parameters and $N_{\rm eff}$, see e.g. [1].

We fix the dark fine structure constant $\alpha_d = 0.007297$ and the mass of dark proton $m_{dp} = 938\,{\rm MeV}/c^2$ to be equal to their light sector values.

This partial opening up of parameter space allows for variation in the redshift of dark recombination $z_{\star d}$, which varies approximately linearly with the ratio $B_d/T_{d\gamma}^0$. For additional description of atomic dark matter parameters, as well as the physics of dark recombination, see [14].

III. DATASETS

In order to constrain the model outlined in Sec. II, this paper utilizes CMB data from *Planck*, namely the *Planck* 2018 high-ℓ TT+TE+EE, low-ℓ EE, low-ℓ TT, and lensing datasets [4]. This paper also combines this data with baryon acoustic oscillation (BAO) data from 6dFGS [17], SDSS MGS [18], and BOSS DR12 [19].

Additionally, we consider models both with and without constraints from big bang nucleosynthesis (BBN) on helium abundance. We also consider models both with

and without the inclusion of the independent measurement of H_0 from SH0ES [6].

The datasets and constraints used in the following analyses to obtain joint constraints on parameter values are summarized in Table I.

IV. CONSTRAINTS PLACED BY CURRENT DATA

We use a modified version of CAMB [14, 20, 21], a publicly available Einstein-Boltzmann solver, to make model predictions and CosmoMC [22] to calculate the posterior probability distributions of the parameters outlined in Sec. II, given the data sets and BBN constraints outlined in Sec. III, using Markov chain Monte Carlo (MCMC) methods.

While we present results for all four scenarios outlined in Sec. III, we emphasize that the BBN-consistent models are most physically accurate and are thus the focus of our analysis.

A. Constraints on $f_{\rm adm}$

Constraints on $f_{\rm adm}$ are presented in left panel of Fig. 2.

For the both BBN-consistent models, low values of $f_{\rm adm}$ are preferred by the data, but higher values are not excluded, and a tail of nonzero posterior probability persists to $f_{\rm adm} > 0.15$. The BBN-consistent model with the SH0ES data has a greater tolerance for higher $f_{\rm adm}$ than the BBN-consistent model without the SH0ES data.

For the BBN-inconsistent model with the SH0ES data, nonzero $f_{\rm adm}$ is preferred by the data. For the BBN-inconsistent model without the SH0ES data, there are two peaks in the $f_{\rm adm}$ posterior probability distribution: one near $f_{\rm adm} = 0$ and one at high $f_{\rm adm}$.

It is apparent that BBN-consistency has a greater impact than the inclusion of the SH0ES data on the constraints on $f_{\rm adm}$. Although none of the four models tightly constrain $f_{\rm adm}$, atomic dark matter is allowed by the data in all four cases, and the BBN-consistent model without the inclusion of the SH0ES data, the most physically realistic model, places the tightest constraints on $f_{\rm adm}$.

Our constraints on $f_{\rm adm}$ are in disagreement with [16], who find that nonzero $f_{\rm adm}$ is preferred with the inclusion of *Planck* 2013 Sunyaev-Zel'dovich (SZ) data [23]. However, we chose not to include this data due to concerns with its validity and are still able to constrain σ_8 (see Sec. IV D and Sec. V). For more information about the decision to exclude the *Planck* SZ data, see e.g. [24].

TABLE I: Summary of datasets and constraints used in this paper. CMB data is from the *Planck* 2018 high-ℓ TT+TE+EE, low-ℓ EE, low-ℓ TT, and lensing datasets [4]; BAO data is from 6dFGS [17], SDSS MGS [18], and BOSS DR12 [19]; and the SH0ES H_0 data is from the measurement in [6]. BBN-consistency indicates constraints on helium abundance from big bang nucleosynthesis (BBN).

Label	Datasets	BBN-consistency?
BBN-consistent, with SH0ES data	*Planck*, BAO, SH0ES	yes
BBN-consistent, without SH0ES data	*Planck*, BAO	yes
BBN-inconsistent, with SH0ES data	*Planck*, BAO, SH0ES	no
BBN-inconsistent, without SH0ES data	*Planck*, BAO	no
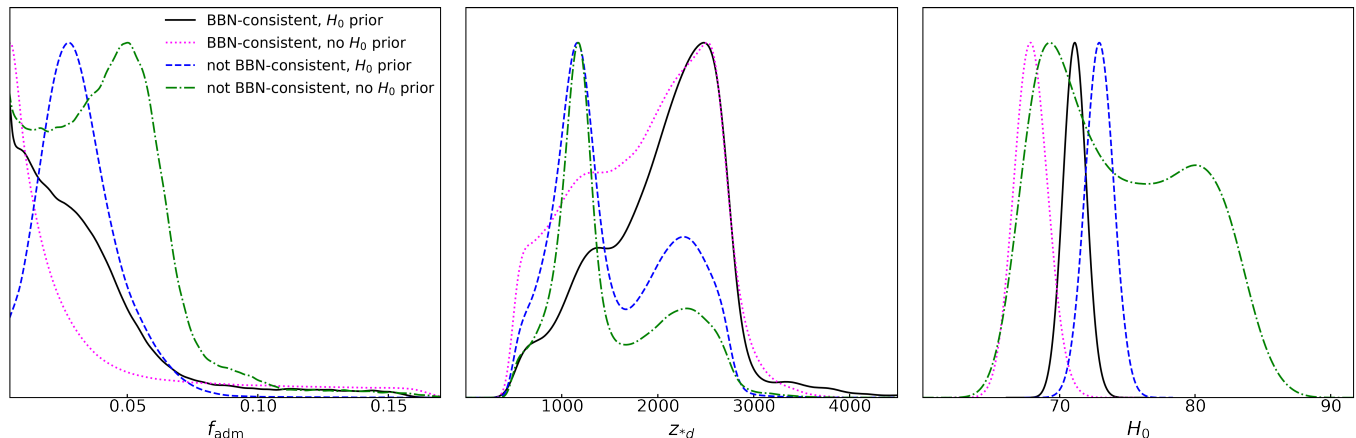
FIG. 2: 1-dimensional posteriors for all four model spaces demonstrating constraints on f_{adm}, $z_{\star d}$, and H_0. The vertical axes indicate probability. "H_0 prior" refers to the inclusion of the SH0ES data, and "no H_0 prior" refers to the exclusion of the SH0ES data.

B. Constraints on $z_{\ast d}$

The constraints on the redshift of dark recombination $z_{\ast d}$ are largely dictated by the prior on the ratio $B_d/T_{d\gamma}^0$, which scales approximately linearly with $z_{\ast d}$ and places an artificial upper limit on $z_{\ast d}$. Comparison of our results to [16] indicate that increasing the upper bound in the prior on $B_d/T_{d\gamma}^0$ (thereby increasing the upper bound on $z_{\ast d}$) may significantly change our results. However, with this caveat, we present our findings for the constraints on $z_{\ast d}$ in the middle panel of Fig. 2.

For both BBN-consistent models, the posterior probability distribution for $z_{\ast d}$ peaks near $z_{\ast d} \approx 2700$, which corresponds to dark recombination occurring before light recombination.

Both BBN-inconsistent models have bimodal posterior probability distributions for $z_{\ast d}$. Both distributions have their primary peak near $z_{\ast d} \approx 1100$, as expected from the scaling symmetry solution in [8] corresponding to dark recombination and light recombination occurring simultaneously. Both BBN-inconsistent posterior distributions have a secondary peak near $z_{\ast d} \approx 2400$.

BBN-consistency has a greater impact than the inclusion or exclusion of the SH0ES data on the posterior distribution for $z_{\ast d}$. While the BBN-inconsistent mod-els place slightly tighter constraints on $z_{\ast d}$, all four of the models place fairly loose constraints on $z_{\ast d}$.

C. Constraints on H_0

The constraints on H_0 are presented in right panel of Fig. 2. As expected, the effects of the SH0ES data are most apparent here, so we will restrict our discussion to the models without the inclusion of the SH0ES data. Although the BBN-consistent model without the SH0ES data peaks at the lowest value of H_0, it holds the most promise for accurately constraining atomic dark matter and offering a solution to existing cosmological tensions. Therefore, we will focus the analysis of constraints on H_0 to this model.

For this BBN-consistent model without the SH0ES data, the H_0 posterior probability distribution peaks at $H_0 = 67.95$ km s^{-1} Mpc^{-1}, which is only slightly higher than the ΛCDM result of $H_0 = (67.49 \pm 0.53)$ km s^{-1} Mpc^{-1} [3–5]. However, tolerance for higher H_0 in line with the SH0ES measurement of $H_0 = (73.04 \pm 1.04)$ km s^{-1} Mpc^{-1} [6] remains. Thus, this partial open-ing of the atomic dark matter parameter space provides a possible solution to the H_0 tension, as seen in [8].

(a) BBN-consistent, with SH0ES data

(b) BBN-consistent, without SH0ES data

(c) BBN-inconsistent, with SH0ES data

(d) BBN-inconsistent, without SH0ES data
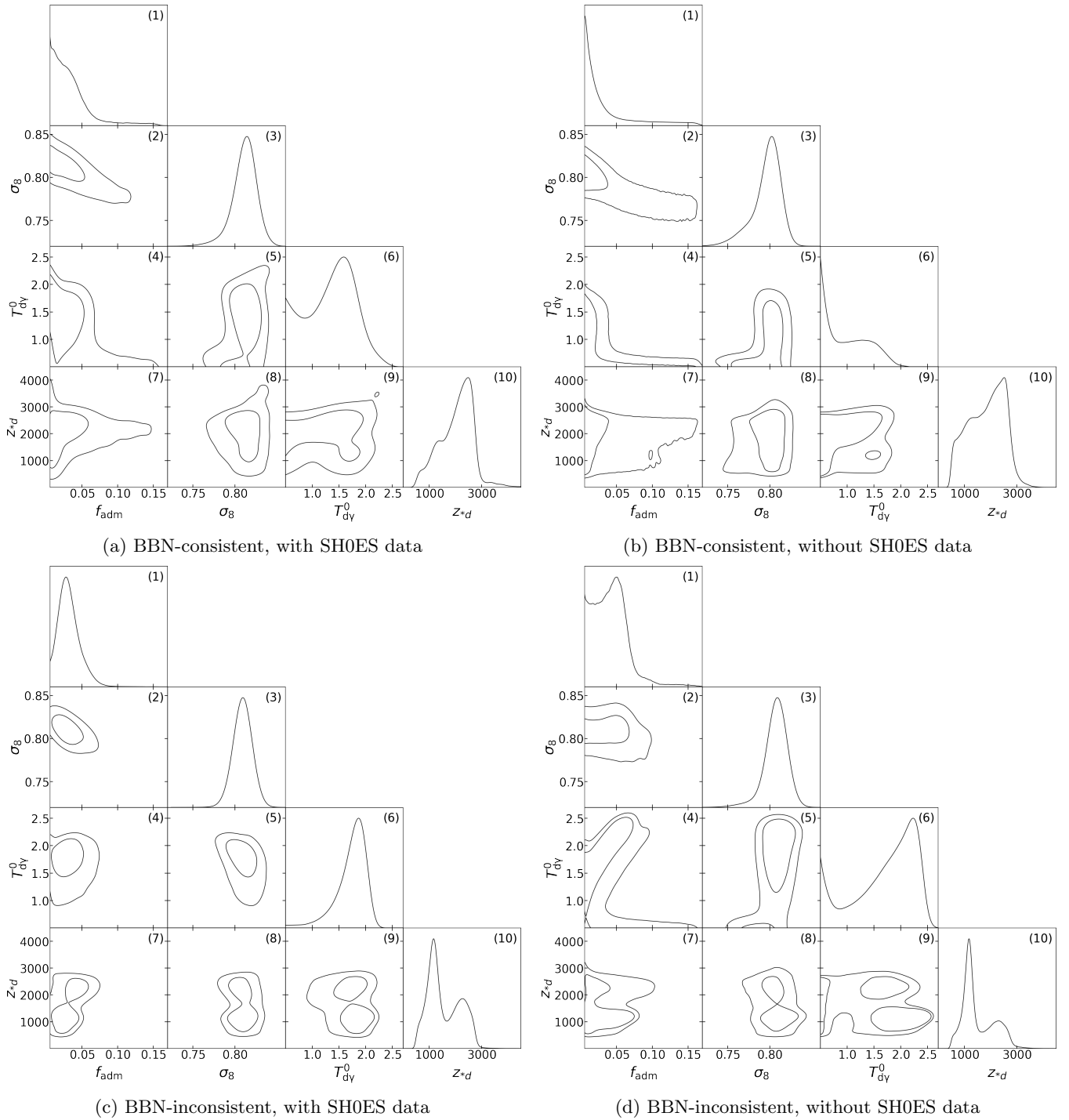
FIG. 3: 1- and 2-dimensional posteriors for f_{adm}, σ_8, $T_{d\gamma}^0$, and z_{*d} for all four model spaces. The vertical axes of the 1-dimensional posteriors along the main diagonals indicate probability. The inner and outer contours on the 2-dimensional posteriors enclose regions of 68% and 95% confidence, respectively.

D. Constraints on σ_8 and $T_{d\gamma}^0$

As can be seen in Fig. 3a(5), 3b(5), and 3d(5), lower values of σ_8 are allowed with lower $T_{d\gamma}^0$. This is unexpected because it would mean that, at low $T_{d\gamma}^0$, atomic dark matter has observational signatures that are distinct from cold dark matter despite the atomic dark matter losing its pressure support much earlier than it would with higher $T_{d\gamma}^0$. This region is especially exciting because it can be seen in three of the four model spaces (all ex-
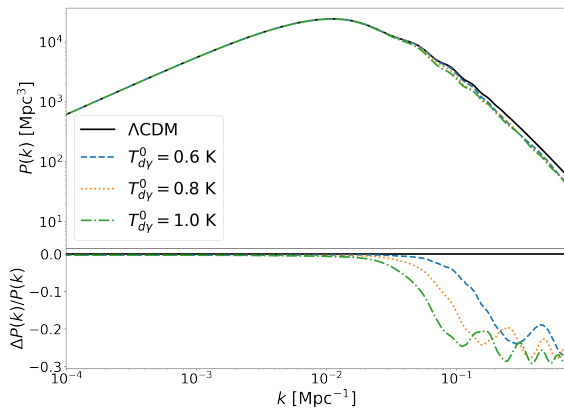
FIG. 4: Linear matter power spectra for a BBN-consistent model with no H_0 prior and fixed $f_{\rm adm} = 0.1$. The solid black line shows the fiducial ΛCDM matter power spectrum, the blue dashed line shows the matter power spectrum for a model with $T_{d\gamma}^0 = 0.6$ K, the orange dotted line shows the matter power spectrum for a model with $T_{d\gamma}^0 = 0.8$ K, and the green dash-dotted line shows the matter power spectrum for a model with $T_{d\gamma}^0 = 1.0$ K.

cept the BBN-inconsistent model with the inclusion of the SH0ES data).

Although the 1-dimensional posterior probability distribution for the BBN-consistent model without the SH0ES data in Fig. 3b(3) peaks at $\sigma_8 = 0.803$, only slightly lower than the ΛCDM value of $\sigma_8 = 0.811 \pm 0.006$ [4], this low σ_8 solution could provide a solution to the σ_8 tension because low $T_{d\gamma}^0$ allows for lower σ_8 closer to the KiDS-1000 result of $\sigma_8 = 0.766_{-0.020}^{+0.025}$ [12], especially for the BBN-consistent model without the SH0ES data that is of greatest interest.

In order to confirm the effects of lower values of σ_8 and verify the observational viability of this possible solution to the σ_8 tension, we will investigate the effects of fixing $f_{\rm adm}$ and varying $T_{d\gamma}^0$ in Sec. V.

V. OBSERVATIONAL VIABILITY OF REGION OF LOW σ_8 AND LOW $T_{d\gamma}^0$

In order to confirm the observational viability and physical effects of the region of low σ_8 and low $T_{d\gamma}^0$ seen in Fig. 3a(5), 3b(5), and 3d(5), we will explore a model with fixed $f_{\rm adm} = 0.1$ and fixed total dark matter $\Omega_c h^2 + \Omega_{db} h^2$. For this model, it can be seen in Fig. 4 that, with increased $T_{d\gamma}^0$, the matter power $P(k)$ is damped relative to the ΛCDM matter power spectrum at higher wavenumber k, while the matter power spectra with nonzero $f_{\rm adm}$ are nearly identical to the ΛCDM matter power spectrum at low k.

However, as can be seen in Fig. 5 and Fig. 6 (note the scale differences on the vertical axes of the residual plots
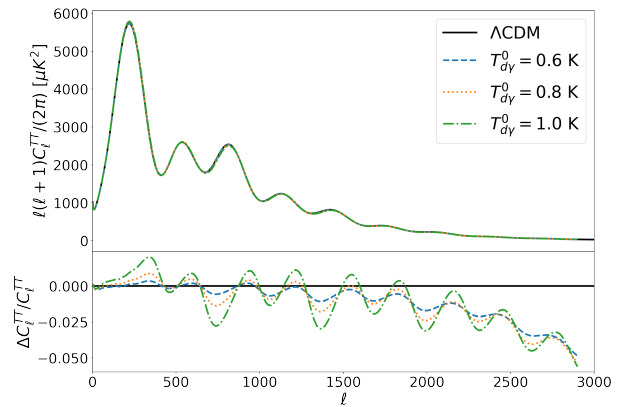
FIG. 5: TT power spectra for same models as in Fig. 4. As in Fig. 4, the solid black line shows the fiducial ΛCDM TT power spectrum, the blue dashed line shows the TT power spectrum for a model with $T_{d\gamma}^0 = 0.6$ K, the orange dotted line shows the TT power spectrum for a model with $T_{d\gamma}^0 = 0.8$ K, and the green dash-dotted line shows the TT power spectrum for a model with $T_{d\gamma}^0 = 1.0$ K.
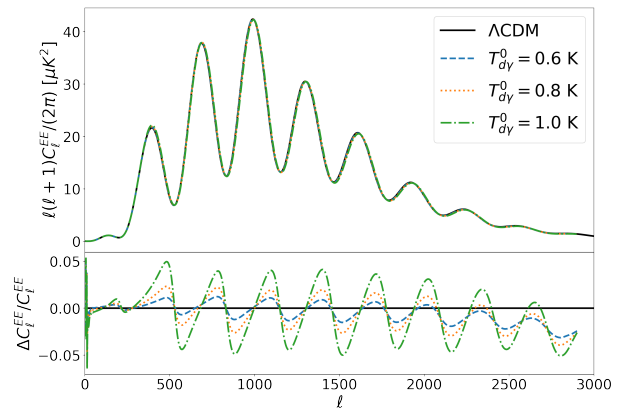
FIG. 6: EE power spectra for same models as in Fig. 4 and Fig. 5. As in Fig. 4 and Fig. 5, the solid black line shows the fiducial ΛCDM EE power spectrum, the blue dashed line shows the EE power spectrum for a model with $T_{d\gamma}^0 = 0.6$ K, the orange dotted line shows the EE power spectrum for a model with $T_{d\gamma}^0 = 0.8$ K, and the green dash-dotted line shows the EE power spectrum for a model with $T_{d\gamma}^0 = 1.0$ K.

between Fig. 4 and Fig. 5/Fig. 6), at fixed $f_{\rm adm}$, the CMB TT and EE power spectra remain nearly unchanged with changing $T_{d\gamma}^0$.

Since $P(k)$ changes while the TT and EE power spectra remain relatively unchanged, we can confirm that changes in $T_{d\gamma}^0$ at fixed fixed $f_{\rm adm}$ do indeed correspond to changes in σ_8 via Eq. 1, as suggested in Fig. 3b. Further, we can conclude that this region of low σ_8 and low $T_{d\gamma}^0$ is in fact observationally viable, as indicated by the constraints placed by current data in Sec. IV D. Thus,

this region of low σ_8 with low $T_{d\gamma}^0$ provides a possible solution to the σ_8 tension.

VI. CONCLUSIONS

Although atomic dark matter is not tightly constrained by current data, it is not excluded and is an observationally viable extension to ΛCDM. In some models, nonzero $f_{\rm adm}$ is preferred by the data, but, in all cases, nonzero $f_{\rm adm}$ is allowed by current data (see the left panel of Fig. 2).

The tolerance for high H_0 for the BBN-consistent model without the SH0ES H_0 data confirms that atomic dark matter can provide a solution to the H_0 tension [8].

Further, we find that low values of σ_8 are allowed with low dark photon temperature $T_{d\gamma}^0$. This allowed region represents an unexpected possible solution to the σ_8 tension with atomic dark matter.

Future directions include a full exploration of parameter space to include variations in the mass of the dark proton m_{dp} and the dark fine structure constant α_d. Other works that have explored the full atomic dark matter parameter space [16] have failed to discover our low σ_8 and low $T_{d\gamma}^0$ solution, so future work is required to understand this discrepancy.

Additional future directions include forecasting the sensitivity of future CMB experiments to atomic dark matter.

VII. ACKNOWLEDGEMENTS

[1] N. Aghanim *et al.* (Planck Collaboration), *Planck* 2018 results: VI. Cosmological parameters, Astronomy & Astrophysics **641**, A6 (2020).

[2] E. W. Kolb and M. S. Turner, *The Early Universe*, Frontiers in Physics No. 69 (Addison-Wesley, Reading, MA, 1990).

[3] L. Balkenhol *et al.* (SPT-3G Collaboration), Constraints on ΛCDM extensions from the SPT-3G 2018 EE and TE power spectra, Physical Review D **104**, 083509 (2021).

[4] N. Aghanim *et al.* (Planck Collaboration), *Planck* 2018 results: V. CMB power spectra and likelihoods, Astronomy & Astrophysics **641**, 10.1051/0004-6361/201936386 (2020).

[5] S. Aiola, E. Calabrese, L. Maurin, S. Naess, and B. L. Schmitt *et al.*, The Atacama Cosmology Telescope: DR4 maps and cosmological parameters, Journal of Cosmology and Astroparticle Physics **2020** (12), 047.

[6] A. G. Riess *et al.*, A Comprehensive Measurement of the Local Value of the Hubble Constant with 1 km s^{-1} Mpc^{-1} Uncertainty from the Hubble Space Telescope and the SH0ES Team, The Astrophysical Journal Letters **934**, 10.3847/2041-8213/ac5c5b.

[7] A. Adil, A. Albrecht, and L. Knox, Quintessential Cosmological Tensions (2022), arXiv:2207.10235.

[8] F.-Y. Cyr-Racine, F. Ge, and L. Knox, Symmetry of Cosmological Observables, a Mirror World Dark Sector, and the Hubble Constant, Physical Review Letters **128**, 201301 (2022).

[9] L. Verde, T. Treu, and A. G. Riess, Tensions between the early and late Universe, Nature Astronomy **3**, 891 (2019).

[10] A. G. Riess, The expansion of the Universe is faster than expected, Nature Reviews Physics **2**, 10 (2019).

[11] E. Abdalla *et al.*, Cosmology intertwined: A review of the particle physics, astrophysics, and cosmology associated with the cosmological tensions and anomalies, Journal of High Energy Astrophysics **34**, 49 (2022).

[12] C. Heymans *et al.*, KiDS-1000 Cosmology: Multi-probe weak gravitational lensing and spectroscopic galaxy clustering constraints, Astronomy & Astrophysics **646**, A140 (2021).

[13] E. Di Valentino *et al.*, Cosmology intertwined III: $f\sigma_8$ and S_8, Astroparticle Physics **131**, 102604 (2021).

[14] F.-Y. Cyr-Racine and K. Sigurdson, Cosmology of atomic dark matter, Physical Review D **87**, 103515 (2013).

[15] F. Ge, F.-Y. Cyr-Racine, and L. Knox, Scaling Transformations and the Origins of Light Relics Constraints from Cosmic Microwave Background Observations (2022), arXiv:2210.16335.

[16] S. Bansal, J. Barron, D. Curtin, and Y. Tsai, Precision Cosmological Constraints on Atomic Dark Matter (2022), arXiv:2212.02487.

[17] F. Beutler, C. Blake, M. Colless, D. H. Jones, L. Staveley-Smith, L. Campbell, Q. Parker, W. Saunders, and F. Watson, The 6dF Galaxy Survey: baryon acoustic oscillations and the local Hubble constant, Monthly Notices of the Royal Astronomical Society **416**, 3017 (2011).

[18] A. J. Ross, L. Samushia, C. Howlett, W. J. Percival, A. Burden, and M. Manera, The clustering of the SDSS DR7 main Galaxy sample – I. A 4 per cent distance measure at $z = 0.15$, Monthly Notices of the Royal Astronomical Society **449**, 835 (2015).

[19] S. Alam *et al.*, The clustering of galaxies in the completed SDSS-III Baryon Oscillation Spectroscopic Survey: cosmological analysis of the DR12 galaxy sample, Monthly Notices of the Royal Astronomical Society **470**, 2617 (2017).

[20] A. Lewis, A. Challinor, and A. Lasenby, Efficient Computation of Cosmic Microwave Background Anisotropies in Closed Friedmann-Robertson-Walker Models, The Astrophysical Journal **538**, 473 (2000).

[21] F.-Y. Cyr-Racine, R. de Putter, A. Raccanelli, and K. Sigurdson, Constraints on Large-Scale Dark Acoustic Oscillations from Cosmology, Phys. Rev. D **89**, 063517 (2014), arXiv:1310.3278 [astro-ph.CO].

[22] A. Lewis and S. Bridle, Cosmological parameters from CMB and other data: A Monte Carlo approach, Physical Review D **66**, 103511 (2002).

[23] P. A. R. Ade *et al.* (Planck Collaboration), *Planck* 2013 results. XX. Cosmology from Sunyaev–Zeldovich cluster counts, Astronomy & Astrophysics **571**, A20 (2014).

[24] Z. Pan, M. Kaplinghat, and L. Knox, Searching for signatures of dark matter-dark radiation interaction in observations of large-scale structure, Physical Review D **97**, 103531 (2018).